J. Mt. Sci. (2014) 11(5): 1192-1207 e-mail: jms@imde.ac.cn http://jms.imde.ac.cn
DOI: 10.1007/s11629-013-2932-x

Deforestation Trends and Spatial Modelling of its Drivers in the Dry Temperate Forests of Northern Pakistan – A Case Study of Chitral

Khuram Shehzad[1], Faisal M. Qamer[1*], MSR Murthy[1], Sawaid Abbas[2], Laxmi D. Bhatta[1]

1 International Centre for Integrated Mountain Development (ICIMOD), GPO Box 3226, Kathmandu 44700, Nepal

2 The Hong Kong Polytechnic University, Hung Hom, Kowloon, Hong Kong, China

**Corresponding author, e-mail: faisal.qamer@icimod.org; Tel: +977-1-5003222; Fax: +977-1-5003277.*
First author, e-mail: kshehzad@icimod.org; Third author, e-mail: msrmurthy@icimod.org;
Fourth author, e-mail: Sawaid.abbas@connect.polyu.hk; Fifth author, e-mail: lbhatta@icimod.org

Citation: Shehzad K, Qamer FM, Murthy MSR, et al. (2014) Deforestation trends and spatial modelling of its drivers in the dry temperate forests of northern Pakistan – A case study of Chitral. Journal of Mountain Science 11(5). DOI: 10.1007/s11629-013-2932-x

Abstract: Deforestation is a major environmental challenge in the mountain areas of Pakistan. The study assessed trends in the forest cover in Chitral tehsil over the last two decades using supervised land cover classification of Landsat TM satellite images from 1992, 2000, and 2009, with a maximum likelihood algorithm. In 2009, the forest cover was 10.3% of the land area of Chitral (60,000 ha). The deforestation rate increased from 0.14% per annum in 1992–2000 to 0.54% per annum in 2000–2009, with 3,759 ha forest lost over the 17 years. The spatial drivers of deforestation were investigated using a cellular automaton modelling technique to project future forest conditions. Accessibility (elevation, slope), population density, distance to settlements, and distance to administrative boundary were strongly associated with neighbourhood deforestation. A model projection showed a further loss of 23% of existing forest in Chitral tehsil by 2030, and degradation of 8%, if deforestation continues at the present rate. Arandu Union Council, with 2212 households, will lose 85% of its forest. Local communities have limited income resources and high poverty and are heavily dependent on non-timber forest products for their livelihoods. Continued deforestation will further worsen their livelihood conditions, thus improved conservation efforts are essential.

Keywords: Remote sensing; Drivers of deforestation; Cellular automata

Received: 20 November 2013
Accepted: 4 August 2014

Introduction

Forests play a critical role in regulating the Earth's surface temperature and precipitation, preserving soil nutrients, minimizing flooding, and fixing carbon. They also provide important ecosystem services to people such as air purification, erosion control, and biological reservoirs. There is a continuing decline in forest area worldwide; the global assessment reported a 0.2% annual loss of forest area between 1990 and 2000, although forest protection efforts reduced the deforestation rate to 0.13% between 2000 and 2005 (FAO 2010).

There are various hot spots of deforestation, one of which is Pakistan, which has the second highest deforestation rate in Asia (Tole 1998; FAO 2010). National level assessments reported 4.2 million ha of forest cover in Pakistan in 1990, or

4.8% of the total land area (GoP 1992), with a rate of loss of 0.7% per annum during 1990–2000 (GoP 2004). The FAO reported that the rate of loss was 1.6% per annum in 1990–2000 and that this rose to 2.0% per annum in 2000–2010 (FAO 2010). The forests are vital both for local communities and the broader environment of the country, but these alarming rates of deforestation raise the question of how long these rapidly vanishing forests can be sustained.

The environmental losses due to deforestation in the Himalayan mountains go beyond the region and badly affect the environment and economy of the adjoining Indo-Gangetic plains area through disturbances in the hydrological cycle and impacts related to soil erosion, siltation, floods, and desertification (Swaminathan 1988; Tiwari 2000). The incidence of floods in the Indus river system has been more severe and more frequent over the past 25 years than in the previous 65 years, mainly due to increased surface runoff and accelerated erosion in the Himalayan mountains (Tejwani 1990). According to the Pakistan Water Strategy, the country needs to increase water storage by 18 million acre-feet (MAF) [22.20 cubic kilometre] by 2050, with 30 percent of this to replace storage lost due to siltation (GoP 2002).

A number of studies have assessed changes in the area of Himalayan dry temperate forests using coarse and high-resolution remote sensing data (Shroder 1998; Joshi Joshi et al. 2001; Gairoal 2004; Pandit et al. 2007). Others have assessed the extent and evaluated the drivers of deforestation (Ali et al. 2005; Qasim et al. 2011; Qamer et al. 2012). Driving forces are the forces that cause observed landscape change, i.e., they are influential processes in the evolutionary trajectory of the landscape (Bürgi 2004). It is important to understand past and present drivers of landscape change in order to design interventions to reduce negative developments. Verburg (1999) modelled land use change as a function of the drivers, thus enabling better understanding of the extent and location of land use change and its effects. Deforestation results from complex socioeconomic processes and it is often difficult to isolate a single cause (Walker 1987; Geist and Lambin 2001). According to the conceptual framework developed by Geist and Lambin (2001), the direct causes of deforestation are expansion of infrastructure and agriculture, extraction of wood, and other factors, including pre-disposing biophysical condition and social trigger events. This framework was used by Rademaekers et al. (2010) in a global study on the evolution of drivers of deforestation and their potential impacts on the cost of schemes for avoiding deforestation. Similarly, Hosonuma et al. (2012) identified expansion of agriculture and timber extraction as the most prominent causes of deforestation and forest degradation in developing countries, including Pakistan. Environmental factors, including geology, topography, and soil quality, and climatic factors such as drought, are also believed to strongly affect deforestation (Geist and Lambin 2001; Chomitz and Thomas 2003). However, most of the deforestation studies that mention environmental factors focus primarily on soil-related features (Fearnside 1993; Geist and Lambin 2001). Studies in Pakistan have identified different drivers, agricultural expansion and population growth are mentioned most frequently (Schickhoff 1995; Lodhi et al. 1998; Nüsser 2000; Qasim et al. 2011), other drivers include timber extraction, poverty, administrative reforms, and poor management (Knudsen and Madsen 1999; Ali et al. 2005; Qamer et al. 2012).

Although survey data are useful for identifying socioeconomic factors, they can only offer a limited view of land cover in a limited area at a particular point in time. In contrast, aerial and satellite imagery can be used to monitor large areas and the spatial extent of changes. Satellite imagery offers contiguous spatial coverage, facilitates better repetition, replaces costly and slow data collection, and provides statistical information about the area or object. Specifically, remote sensing change detection analysis can be used to identify areas of rapid change to target management efforts (Rogan and Roberts 2002; Kennedy 2009; Henders and Ostwald 2012). Repeated satellite images are useful both for visual assessment of natural resources dynamics occurring at a particular time and place, and for quantitative evaluation of land cover changes (Tekle 2000).

Studying driving forces is more problematic; there is no single method, but the roots of the different methods are basically the same (Bürgi 2004). There are various models available each with specific advantages and disadvantages (Agarwal 2002). One modelling approach, the cellular automaton, works synchronously according to a simple set of rules depending only on the local information provided by the states of neighbouring cells (Kutrib 1997). Wolfram (1983) refers to nearly 50 papers related to applications of cellular automata, indicating the model's accuracy and reliabi lity. Soares-Filho et al. (2006) used a similar approach for modelling deforestation trends in the Amazon basin, as Geri et al. (2011), Kamusoko et al. (2011), Maeda et al. (2011) and Farfán (2012) did in their studies of land cover change including deforestation.

The aim of the current study was to assess deforestation in Chitral, Pakistan, to model the contribution of spatially explicit drivers of deforestation, and to project the future forest scenario on a business as usual basis. Future forest projection has not been done previously for dry temperate forests in the western Himalayan mountain areas. The study used supervised classification of Landsat satellite images for forest cover mapping and employed a cellular automaton modelling technique for spatial modelling of forest cover change dynamics.

1 Study Area

Chitral tehsil is a sub-district administrative unit of 5818 km² in the extreme northwest of Pakistan, surrounded by the glaciated mountain ranges of the Hindu Raj to the south and the Hindu Kush to the west and north (Khan 1975; Malik 1985), and ranging in elevation from 1063 to 6628 m asl (Figure 1). The Hindu Kush climate is marked by the transition from the west (dry) to the south (moist) Asian climatic zone and its inner valleys are in a rain shadow. The climate in Chitral is temperate and is dominated by the winter weather pattern with rain-bearing westerly winds from December to March. The mean annual temperature is 16°C, with an average minimum temperature of 8°C and average maximum temperature of 24°C. Summers are hot with July the hottest month, and winters cold with January the coldest month (Beg 1974). Temperatures in winter can drop to -3°C (absolute minimum) and in the summer can reach 47°C (absolute maximum). The average annual rainfall is 451 mm, with heavy snowfall in winter. The vegetation is characterized as dry temperate with three dominant vegetation types – dry temperate oak forest, dry temperate coniferous forest, and alpine meadow (Champion et al. 1966). Deodar (*Cedrus deodara*) is the dominant species in coniferous forest, and oak (*Quercus baloot*) and walnut (*Juglans regia*) in broadleaved forest (Sheikh and Khan 1983).

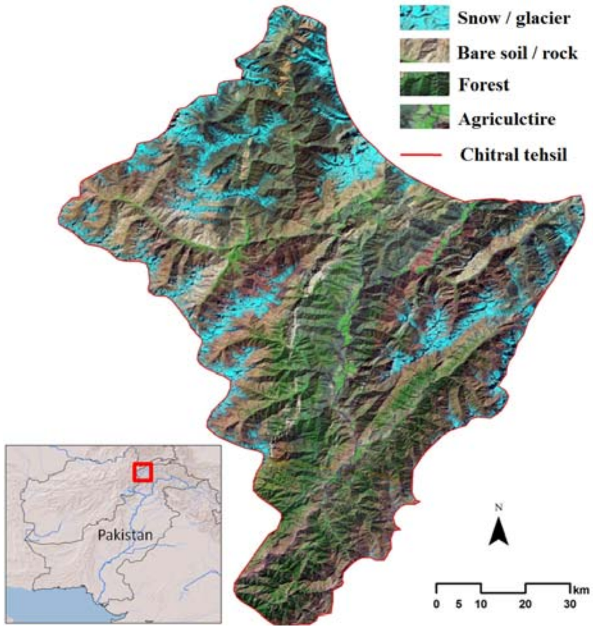

Figure 1 Study area map.

2 Materials and Methods

2.1 Forest cover classification and change analysis

We utilized Landsat satellite images captured on 27/Sep/1992, 27/Oct/2000, and 10/Sep/2009 to develop time series land cover maps. The datasets were selected on the basis of similar seasonality and minimum cloud cover. Satellite data with six spectral bands of the same spatial resolution (30 m) were stacked and then masked to the study area. It is difficult to obtain consistent classes from images of the same location taken at different dates as a result of differences in illumination, atmospheric effects, and instrumental response (Adams et al. 1995). To maintain consistency between the classes, radiometric atmospheric correction was carried out by converting the satellite-generated digital counts

(DC) to absolute surface reflection (Chavez 1996), and then images were geometrically corrected and rectified taking historic images as reference with a root mean square (RMS) error of less than 3.35 m. The objective of geometric correction was to bring adjacent images into registration and to overlay different images of the same area from different dates and sensors (Kardoulas et al 1996). Images were further enhanced by applying a standard deviation stretch which enhanced the distinctions between the features. Using field expertise, a training sample was identified for 13 land cover classes and each class was analyzed for spectral behaviour using different band combinations (Table 1).

After identifying signatures for the land cover classes, maximum likelihood supervised classification was applied using feature space with a non-parametric decision rule. Maximum likelihood supervised classification has been used in many studies, for example Keuchel et al. (2003) and Rozenstein and Karnieli (2011). Gong et al. (2003) further improved land cover outputs using supervised classification by including detailed vegetation indices given by elevation, slope, and aspect. A fuzzy filter with a 3 × 3 window was applied on the final outputs for smoothing. The resolution of the final land cover was 90 m; each pixel of the land cover dataset covered an area of 0.81 ha.

The land cover was primarily classified into 13 classes (Table 1) including six forest cover classes (dense coniferous forest, sparse coniferous forest , dense mixed forest, sparse mixed forest, sparse broadleaved forest) and seven non-forest cover classes (grassland/shrubs, peatland, alpine grassland, agriculture, bare soil/rocks, snow/glaciers/ice, water bodies). Transition from forest to non forest was taken as deforestation and dense forest to sparse forest was taken as degradation. Change in forest cover classes was quantified using the output layers of land cover for three different years and cross tabulation between layers using the spatial analysis tool in ArcGIS. Changes other than forest were neglected because of the complexities of seasonal variation. The peak season for grasses, shrubs, peatland, and alpine grass is just after the monsoon, snowfall has a maximum in winter, and agricultural types vary across all seasons. Forest cover change from 1992 to 2000 was taken as the initial landscape change, and from 2000 to 2009 as land cover inputs for the model. No regeneration was identified on the land deforested between 1992 and 2000, thus the deforested land in the final landscape was the sum of the deforestation over the two periods.

The accuracy of the land cover maps developed from Landsat satellite images was assessed by comparing the land cover results with Google Earth based very high resolution satellite (VHRS) images.

Table 1 Description of Land Cover Classes

	Land cover class	Description
1	Dense coniferous forest	Dense evergreen needle-leaved forest with canopy cover greater than 60%, mainly includes moist and dry temperate Himalayan forest, sub-alpine forest, and sub tropical pine forest
2	Sparse coniferous forest	Sparse evergreen needle-leaved forest with canopy cover less than 60% mixed with scrub, bare areas, and grasses/shrubs
3	Dense mixed forest	Mixed forest of evergreen needle-leaved, broadleaved, and scrub forest with density greater than 60%
4	Sparse mixed forest	Sparse coniferous, broadleaved, and scrub forest with canopy cover less than 60% mixed with scrub, bare areas, and grasses/shrubs
5	Dense broadleaved forest	Dense broadleaved and scrub forest with canopy cover greater than 60%
6	Sparse broadleaved forest	Sparse broadleaved and scrub forest with canopy cover less than 60% mixed with scrub, bare areas, agriculture, and grasses/shrubs
7	Grassland/shrubs	Grasses and shrubs, which are hard to differentiate because of the limitations of spatial resolution, and the fact that shrub in the upper mountain regions of Pakistan mainly consists of dwarf shrubs mixed with grasses
8	Alpine grassland	Alpine pasture above 4000 masl elevation
9	Peatland	Naturally accumulated layer of peat mixed with standing water, mostly found at high elevation
10	Agriculture	Crop-bearing or harvested fields depending upon the season of the scene
11	Bare soil/rock	Non-vegetated areas including river sand, mud, barren land, and rocks
12	Snow/glaciers/ice	Includes both perennial and non-perennial snow and ice
13	Water bodies	Includes both small and large tributaries which can be classified, and standing water (lakes and dams)

A total of 200 stratified random samples were selected from the VHRS images and the validation sample points overlaid on the land cover map. Systematic accuracy assessment was mainly carried out for the land cover map of 2009 as most of the Google Earth images were from 2007 to 2010. All the major land cover changes, particularly deforestation, were again verified in the Google Earth images.

2.2 Model setup and calibration

2.2.1 Selection of landscape variables

Deforestation and degradation were taken as the response variables. Explanatory variables (drivers) were chosen based on a literature review (Schickhoff 1995; Lodhi et al. 1998; Knudsen and Madsen 1999; Nüsser 2000; Geist and Lambin 2002; Ali et al. 2005; Qasim et al. 2011; Hosonuma et al. 2012) as well as data availability and quality; initially thirteen static explanatory landscape variables were considered (Table 2, Figure 2). To understand the forest structure complexity, we also used distance to perforation and distance to edge of forest within the biophysical category. Perforation refers to the forest pixels that define the boundary between core forest and relatively small clearings (perforations) within the forested landscape. These values are static and remain the same in all iterations of the model. The distance to previous deforestation and distance to previous degradation were taken as dynamic variables which change their value with each iteration of the model.

Continuous raster variables (as per software requirement) such as the distance to agricultural land or elevation were categorized using Jenks' optimization method (natural breaks). The only major drawback with this method is that the number of classes has to be defined first and the number of classes depends on the detail of the data available. An over or underestimation of the weights can occur if the explanatory variables are not independent, which could affect the analysis. Spatial dependency between the drivers was tested by calculating correlations between the variables. We tested the correlation between the drivers with three tests: Cramer's coefficient, contingency, and uncertainty joint information. Cramer's coefficient and contingency were derived from chi-square, and uncertainty joint information from joint entropy (Almeida2005; Maeda 2011).

The model was implemented using Dinamica EGO freeware (Soares-Filho et al. 2013) (csr.ufmg.br/dinamica) and Excel Software, and processing was performed using the computing resources of the SERVIR-Himalaya programme (https://www.servirglobal.net/Himalaya/about.aspx) at the International Centre for Integrated Mountain Development (Kathmandu, Nepal).

2.2.2 Transition rates and probabilities

To understand the forest cover change dynamics, the state and transitions of forest cover were classified into five categories: dense forest,

Table 2 Landscape Variables

Variable	Source
Biophysical	
Elevation	Freely downloaded ASTER DEM
Slope	Extracted using DEM
Aspect	Extracted using DEM
Distance to perforated areas	Extracted using forest fragmentation
Distance to edges	Extracted using forest fragmentation
Socioeconomic	
No. of households	Population census carried out by Agha Khan Rural Support Programme for the Benazir Income Support Programme (BISP) 2008.
Population density	Population census carried out by Agha Khan Rural Support Programme for the Benazir Income Support Programme (BISP) 2008.
Management	
Distance to protected areas	World Conservation Monitoring Centre.(http://www.protectedplanet.net/)
Distance to settlements	Survey of Pakistan map sheets. (http://www.surveyofpakistan.gov.pk/)
Distance to administrative boundary	Survey of Pakistan map sheets. (http://www.surveyofpakistan.gov.pk/)
Distance to agricultural land	Extracted using land covers of 2009

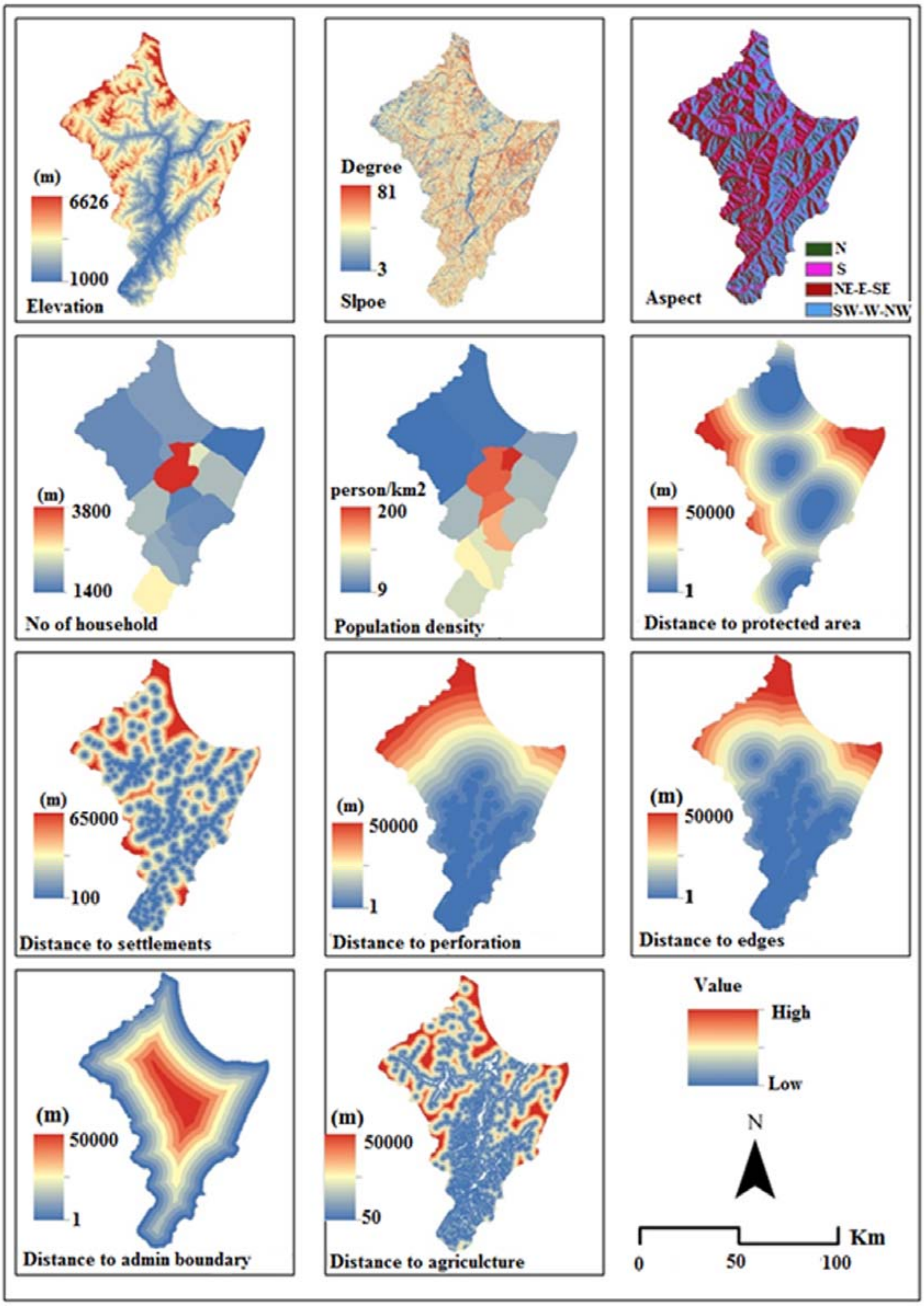

Figure 2 Maps of landscape variables (spatially explicit drivers).

sparse forest, dense forest to non-forest (deforestation), dense forest to sparse forest (degradation), and non-forest. The amount of regeneration was extremely small (8 ha), thus transitions of non-forest to forest, or sparse forest to dense forest, were ignored in the model. The status of forest cover 1992 and changes until 2000 were taken as the initial landscape and changes in the forest between 2000 and 2009 as the final landscape. Transition rates were calculated by cross tabulation of land cover layers between 1992 and 2009, which refers to the amount of change for each land cover class for the particular simulation period. The transition rate per year for each class was obtained by dividing the total transition rate with the total number of time steps.

A transition rate matrix with the converted categorical variables was used as the input to calculate the probabilities for each transition. The probabilities for each cell for every transition were calculated using the weight of evidence method (Goodacre 1993; Bonham-Carter 1994). The weight of evidence is a Bayesian method in which the effect of each landscape variable on a transition is calculated independently of the combined solution (Soares-Filho et al. 2002; Maeda 2011). A more detailed explanation of the statistical formula used to calculate spatial probability can be found in Agterberg and Bonham-carter (1990), Goodacre (1993), Bonham-Carter (1994), and Maeda (2011).

Validation is concerned with how well the model outcomes represent real system behaviour and involves comparing model outputs with real-world observations or the product of another model or theory assumed to adequately characterize reality (Parker 2008). The validation process model space must be made by methods of comparison based on proximity, since pixels do not coincide cell by cell but may have patterns of similarity. We used the Dinamica calc reciprocal similarity function, which is a modified version of the function used by Pontius (2002). Predicted landscape and observed landscape are the inputs for validation, while the output is a model fitness curve, which varies with window size. We used multiple windows and a constant decay function, which measures errors due to location and quantity, for the validating model. Probabilities and a future simulated landscape map for 2030 were produced following completion of the calculations.

3 Results and Discussion

The total accuracy rate (total number of accurate pixels compared to number of pixels taken as reference) was 87.6% and the kappa statistics value 85.0%. The producer's accuracy was over 80% in all classes except agricultural fields (78.9%); the user's accuracy was over 80% in all classes except for grasses (75%). The land cover and land cover change values for 1992, 2000, and 2009 are shown in Table 3.

The crammer's coefficient values between the variables and joint information uncertainty are summarized in Table 4. Values of 0.8 and above are significant and indicate a high correlation. Grey-shaded cells show the results with Cramer's coefficient and the remaining cells the results with joint information uncertainty; significant values are marked red, and mean it is not useful to use both variables. From this, we excluded the number of households, which is highly correlated with population density. We also excluded the distance to edges on the basis of the third test, correlation contingency, which showed a high correlation with distance to perforated areas (value 0.9103) even though the values using Cramer's coefficient and joint information uncertainty were just below 0.8 (Table 4).

Table 3 Land cover and change in 1992, 2000, and 2009 (ha)

Land cover class	1992	2000	2009	Change 1992–2000	Change 2000–2009
Dense coniferous forest	37,134	36,830	35,128	-304	-1702
Sparse coniferous forest	21,958	21,610	20,472	-348	-1138
Dense mixed forest	3369	3382	3167	13	-215
Sparse mixed forest	1293	1230	1232	-63	2
Dense broadleaved forest	0	0	0	0	0
Sparse broadleaved forest	0	2	2	2	0
Grassland/shrubs	123,008	123,081	127,710	73	4,629
Alpine grassland	5699	5517	6007	-182	490
Agriculture	23,276	23,330	14,332	54	-8998
Bare soil/rock	319,413	296,979	342,667	-22,434	45,688
Snow/glaciers/ice	45,945	69,129	29,966	23,184	-39,163
Water bodies	748	753	1,160	5	407
Total area	**581,843**	**581,843**	**581,843**	0	0

Table 4 Cramer's coefficient (shaded grey) and joint information uncertainty values between drivers

	A	B	C	D	E	F	G	H	I	J	K	L	M
A	1		0.046	0.088	0.384	0.402	0.083	0.048	0.003	0.004	0.112	0.297	0.297
B		1	0.070	0.059	0.255	0.307	0.072	0.048	0.003	0.004	0.083	0.400	0.400
C	0.144	0.175	1	0.041	0.084	0.091	0.071	0.036	0.002	0.002	0.041	0.135	0.135
D	0.209	0.176	0.167	1	0.109	0.106	0.031	0.122	0.000	0.011	0.246	0.079	0.079
E	0.372	0.292	0.191	0.245	1	0.576	0.189	0.064	0.002	0.006	0.131	0.300	0.300
F	0.387	0.345	0.213	0.244	0.588	1	0.159	0.074	0.003	0.006	0.148	0.308	0.308
G	0.152	0.145	0.180	0.161	0.299	0.266	1	0.023	0.004	0.003	0.037	0.199	0.199
H	0.167	0.155	0.137	0.280	0.288	0.299	0.108	1	0.001	0.010	0.129	0.056	0.056
I	0.053	0.058	0.042	0.021	0.051	0.060	0.066	0.037	1	0.001	0.001	0.007	0.007
J	0.049	0.050	0.033	0.076	0.059	0.058	0.043	0.077	0.029	1	0.013	0.008	0.008
K	0.240	0.218	0.160	0.363	0.269	0.290	0.156	0.269	0.030	0.091	1	0.114	0.114
L	0.326	0.403	0.283	0.200	0.323	0.335	0.286	0.158	0.091	0.071	0.254	1	1.000
M	0.326	0.403	0.283	0.200	0.323	0.335	0.286	0.158	0.091	0.071	0.254	1.000	1

Notes: A = distance to previous deforestation, B = distance to previous degradation, C = distance to admin boundary, D = distance to agriculture, E = distance to edges of forest, F = distance to perforation areas of forest, G = distance to protected areas, H = distance to settlements, I = aspect, J = slope, K = elevation, L = no. of households, M = population density

Table 5 Change matrix for land cover classes in 1992 and 2000

LC CODE	DCF	SCF	DMF	SMF	SBF	GS	AG	A	BSR	SGI	W	Total 1992
DCF	**36,830**	46				219			39			**37,133**
SCF		**21,564**				358		4	32			**21,958**
DMF			**3311**	34		23			1			**3369**
SMF			69	**1196**		27		1				**1293**
SBF					**0**							**0**
GS			1		2	**121,827**		28	849	292	9	**123,008**
AG							**5480**	1	7	210		**5699**
A						33		**8400**	603	11	99	**23,276**
BSR						589	27	725	**286,925**	30,778	369	**319,413**
SGI						3	8	1	8127	**37,803**	1	**45,945**
W						3	1	39	395	34	**275**	**748**
Total 2000	**36,830**	**21,610**	**3381**	**1230**	**2**	**123,081**	**5516**	**23,329**	**296,979**	**69,129**	**753**	**581,841**

Notes: LC CODE= Land cover code, DCF = dense coniferous forest, SCF = sparse coniferous forest, DMF = dense mixed forest, SMF = sparse mixed forest, SBF= sparse broadleaved forest, GS = grassland/shrubs, AG = alpine grassland, A = agriculture, BSR = bare soil/rocks, SGI = snow/glaciers/ice, W = water bodies

3.1 Forest land cover distribution and spatio-temporal change

In 2009, around 10% (60,001 ha) of the study area was forested. The time series analysis (1992 – 2000 – 2009) revealed considerable deforestation and degradation with 3759 ha of forest area lost in total (6%) over the 17 years, including 1664 ha of dense forest. The annual rate of deforestation increased from 0.14% between 1992 and 2000 to 0.54% between 2000 and 2009 (Table 3, Figure 3a and 3b).

The conversion between classes in the two periods is shown in a change matrix (Tables 5 and 6). The largest conversion of a forest cover class was from sparse coniferous forest to non forest: 394 ha between 1992 and 2000, and 1602 ha between 2000 and 2009. The next largest was from dense coniferous forest to non forest: 258 ha between 1992 and 2000, and 1237 ha between 2000 and 2009. The third largest was from dense coniferous forest to sparse coniferous forest: 46 ha between 1992 and 2000, and 464 ha between 2000 and 2009.

There are 13 administrative subunits (union councils) in Chitral tehsil. The forest cover distribution across the union councils is shown in Figure 4, and the deforestation in each unit in Figure 5. Arandu union council had the greatest area of forest cover (13,801 ha), and also the greatest deforestation and highest rate of deforestation in both periods – 0.39% per annum between 1992 and 2000 and 1.08% per annum between 2000 and 2009 (Figures 4 and 5).

3.2 Non-forest land cover distribution

In 2009, about 2.5% (14,332 ha) of the total area was agricultural land (Table 3). There was a negative trend from 1992 to 2009, which is consistent with the findings of the agricultural census reports (GoP 2010). Around 23% (133,717 ha) of the area was grasses and shrubs, including 1% of alpine grassland; and 59% (342,667) was bare soil and rocks. Snow and glaciers were classified as a single land cover class; they covered about 5% of

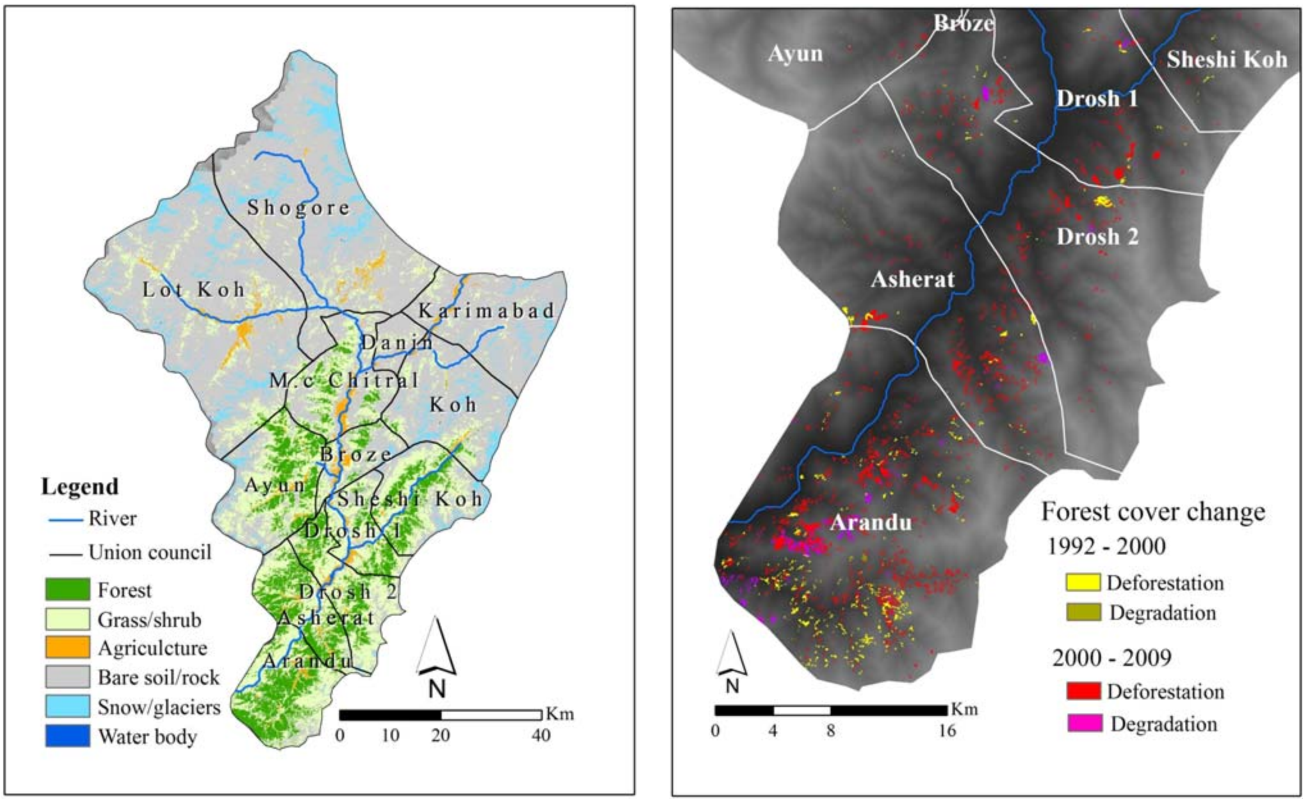

(a) Land cover in 2009

(b) Deforestation and forest degradation from 1992 to 2000 and 2000 to 2009

Figure 3 Land cover in 2009, Deforestaton from 1992 to 2000 and Forest Degradation from 2000 to 2009.

Table 6 Change matrix for land cover classes in 2000 and 2009

LC CODE	DCF	SCF	DMF	SMF	SBF	GS	AG	A	BSR	SGI	W	Total 2000
DCF	**35,128**	464				1,116			121			**36,830**
SCF		**20,008**				896		1	706			**21,610**
DMF			**3156**	79		68			77			**3380**
SMF			7	**1153**		23			47			**1230**
SBF					**2**							**2**
GS			3			**122,533**		58	485		2	**123,081**
AG							**5475**		10	31		**5517**
A						2,551	1	**12,390**	6,722		39	**23,330**
BSR			1			257	1	190	**287,950**	7,963	616	**296,979**
SGI						258	529	3	46,308	**21,971**	60	**69,129**
W						8		61	240		**443**	**753**
Total 2009	**35,128**	**20,472**	**3167**	**1232**	**2**	**127,710**	**6,007**	**14,331**	**342,666**	**29,965**	**1160**	**581,840**

Notes: LC CODE= Land cover code, DCF = dense coniferous forest, SCF = sparse coniferous forest, DMF = dense mixed forest, SMF = sparse mixed forest, SBF= sparse broadleaved forest, GS = grassland/shrubs, AG = alpine grassland, A = agriculture, BSR = bare soil/rocks, SGI = snow/glaciers/ice, W = water bodies

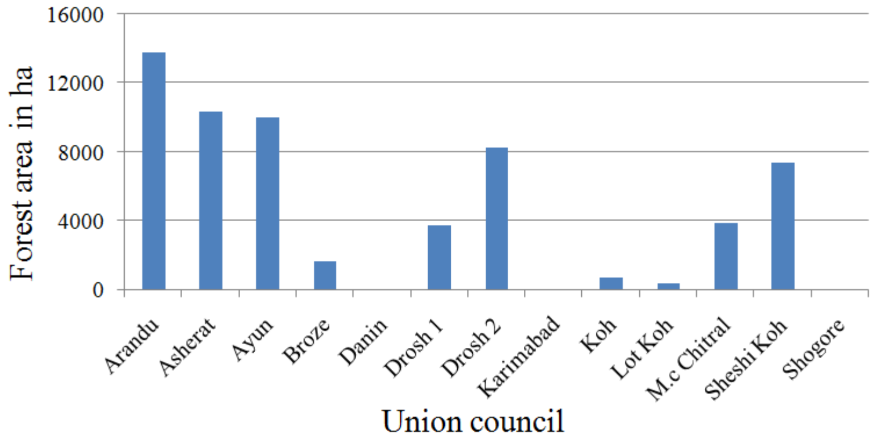

Figure 4 Forest cover distribution in individual union councils in 2009.

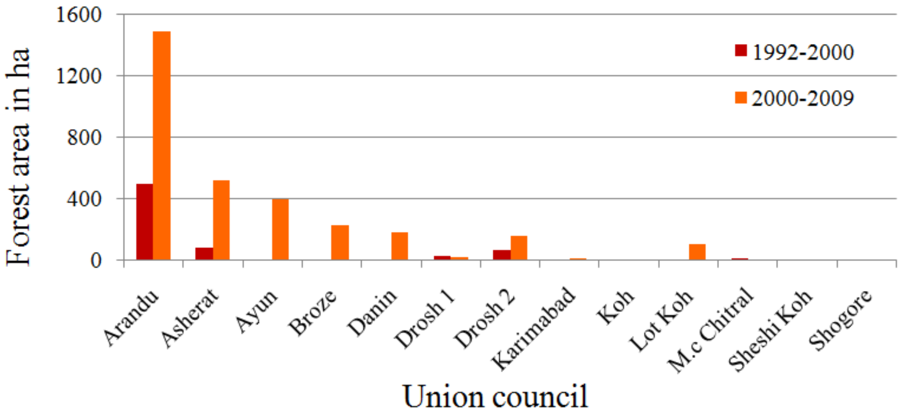

Figure 5 Deforested area in union councils in 1992 to 2000 and 2000 to 2009.

the area (29,966 ha).

Snow and grass cover distribution are highly sensitive to local weather conditions and the limited observations of Landsat images are not sufficient to document the variability. Due to the significant intra-annual changes within grasslands and snow, it was not possible to quantify their explicit conversion to another land cover class. Since the focus of the study was to explore forest dynamics, no extra effort was made in this area.

3.3 Landscape variables and their contribution to deforestation and degradation

Weight of evidence (W of E) analysis was used to measure the association of deforested pixels with the presence of a predictor variable (e.g. distance to road, distance to previous deforestation). If more deforestation pixels occur in a specific spatial configuration then the weight is positive (W+), and if less then it is negative (W-). The variables of aspect, distance to perforated areas, distance to protected areas, and distance to agriculture showed negative or close to zero (perforated areas) or arbitrary (aspect) associations with transitions and were not considered for further analysis. Variables of elevation, slope, population density, distance to settlements, and distance to administrative boundaries, all showed a positive association with deforestation (Figure 6).

Elevation and slope essentially represent terrain accessibility and showed the strongest association with forest disturbance. Elevation

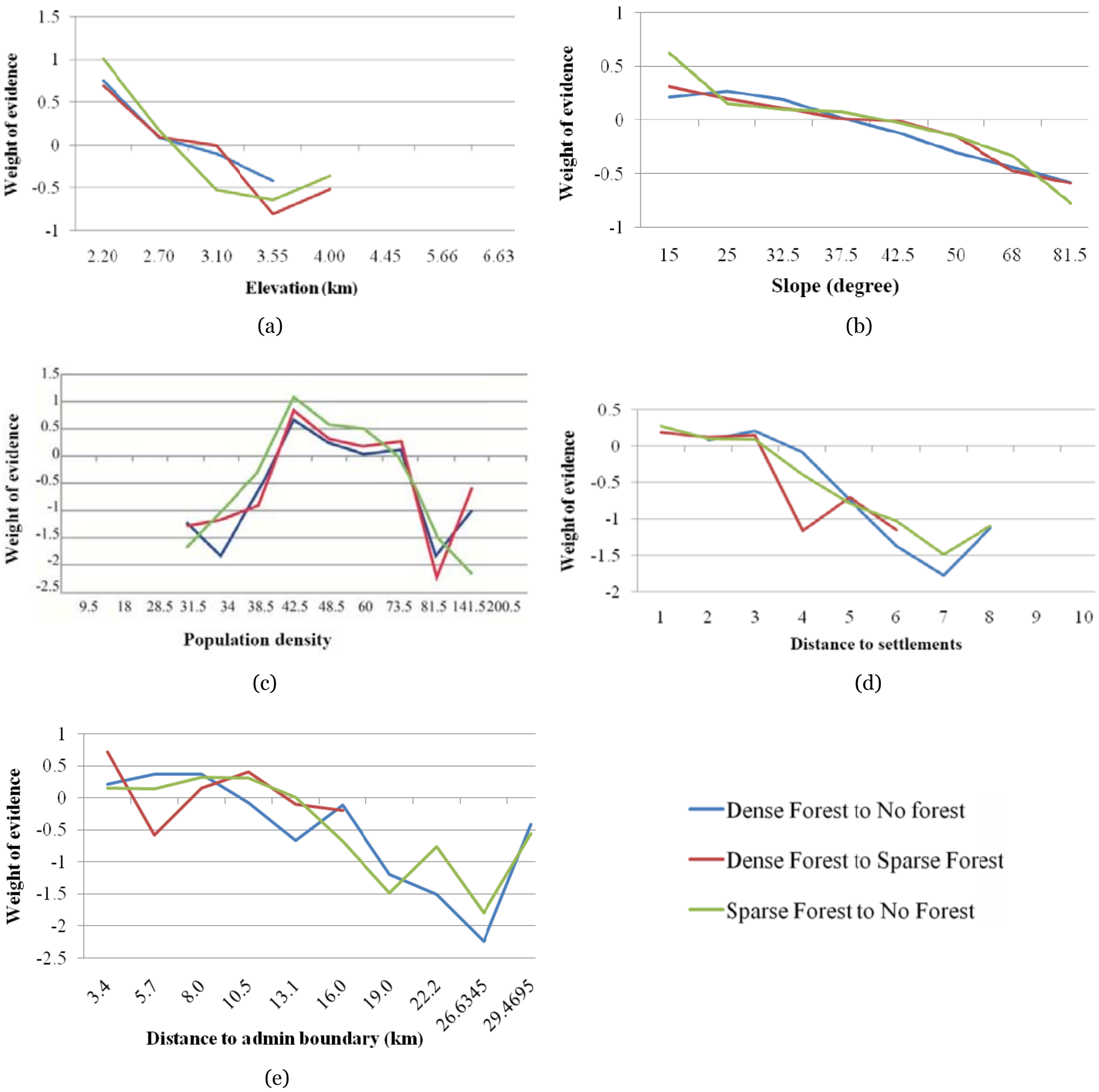

Figure 6 Weight of evidence values of significant deforestation drivers.

<2500 m asl and slope <30° were highly related to deforestation and degradation. High population density was the socioeconomic factor most closely associated with forest transition, with the highest association for a population density of 40 to 60 persons per ha. Higher population density had less effect because the area with high density (Danin union council with ~80 persons per ha) contained very little forest and this very small area remained stable. The main cause of the rapid deforestation and degradation in southern Chitral was the removal of large quantities of firewood. More than half of the firewood used (182,000 m^3, 63% of the total) is taken from the forest, accounting for nearly 60% of the annual growth of all forests in Chitral (NWFP and IUCN 2004). With an annual population growth rate of 2.52% in Chitral district, the situation is likely to worsen if no alternative means of energy supply is provided (GoP 2010).

Among the management variables, distance to settlements and distance to administrative boundary showed the highest correlation with deforestation and degradation. There was almost no forest disturbance within the protected areas, and agricultural encroachment also played a minimal role. The intact forests within the protected area highlight the results of proper management of well-defined legally-protected forests. The lower contribution of agricultural expansion is related to the abandoning of agriculture due to low productivity and labour migration from mountain areas. In Chitral, forests are categorized as Reserve Forests with both management and ownership vested in the state. However, the neighbouring communities have traditional rights and can apply for the use of standing timber for domestic purposes upon payment of a concessionary fee. The high deforestation and degradation rate along the administrative boundaries can probably be attributed to misunderstandings about the jurisdiction of forest areas between forest officials and between communities.

3.4 Model accuracy and future forest scenario

The accuracy of the model is determined by the size of the window, which is variable and can be defined by the user; in this case we chose a maximum window size of 11 × 11. The results of the validation using predicted and observed landscape are shown in Figure 7a. The model achieved a spatial agreement of 74% at a window size of 11 × 11 pixels, which is acceptable based on the results obtained in other studies using cellular automaton methods. According to Novaes et al. (2011), values close to 0.4 indicate a fairly good level of compatibility between the real and the simulated landscape; other studies have achieved values between 0.4 and 0.9, including Ferrari (2008) who obtained 0.44 and 0.84 for dynamic simulation models of land use and land cover, and Benedetti (2010) who achieved levels 0.64 to 0.99 in studies of forest simulation. We also used conventional statistics to compare the simulated forest cover maps for 2009 under the 'business as usual' scenario with the actual (observed) satellite-derived forest cover map for 2009, and thus estimate overall accuracy. For example, the actual dense coniferous forest was 35,128 ha, while the simulated value was 31,722 ha. Visual spatial comparison of the simulated forest cover map and originally observed land cover of 2009 also indicated that the model simulated the forest areas fairly well (Figure 7b).

A simulated forest landscape was prepared for the year 2030 using a 'business as usual' approach (Figure 8). According to the predicted landscape, Chitral tehsil will lose 23% of its forest (in 2009) by 2030 and a further 8% will change from dense forest to sparse forest. Arandu union council, with the greatest extent of forest in 2009, will lose 85% of its forest. The future patterns and trends of deforestation are subject to the conditions of the explanatory variables used during the model calibration and the deforestation rates used in the

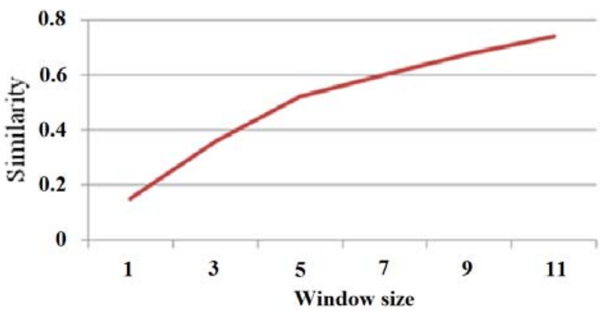

Figure 7a Fuzzy similarity indices based on multiple windows for the simulated landscape 2009. The input land cover resolution was 90 m and the window size 11 pixels so spatial resolution was 990 m.

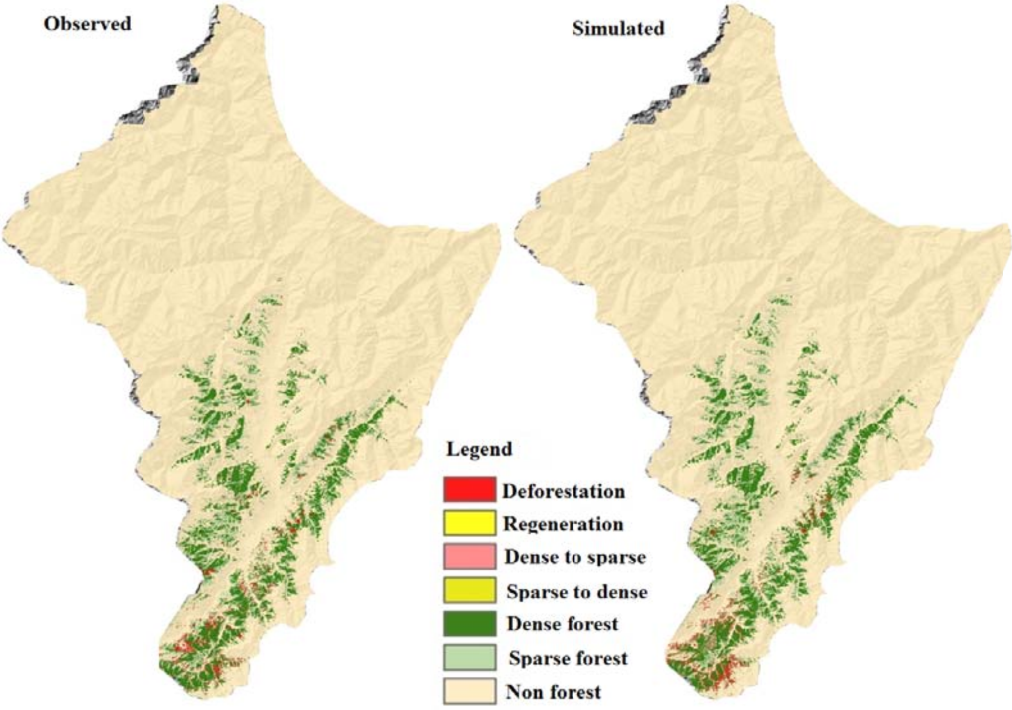

Figure 7b Validation of 2009 predicted forest cover and 2000-2009 forest loss.

simulation.

Chitral in general has high poverty with few income resources; non-timber forest products (NTFPs) are the major source of income and food for the local community. Within the forest ecosystem, neighbouring communities possess the rights to extract wood for fuel, to graze animals, and to harvest various NTFPs including wild mushrooms (*Morchella esculenta, M. vulgaris, M. deliciosa*), honey (from *Apis cerana*), medicinal plants (*Ferula nartex Paeonia emodi, Inula recemosa*, and others), pine nuts (*Pinus gerardiana*), and silk cocoons (Khan 1994). The observed deforestation trends, particularly during the second of the periods studied (2000–2009), and the future projections are alarming, and will cause additional stress to the marginal local communities in the area.

4 Conclusion

The study used remote sensing methods to assess the trends in deforestation in Chitral, northern Pakistan, and models drivers of deforestation to develop future projections. Up to now, forest forecasts have mostly been concerned

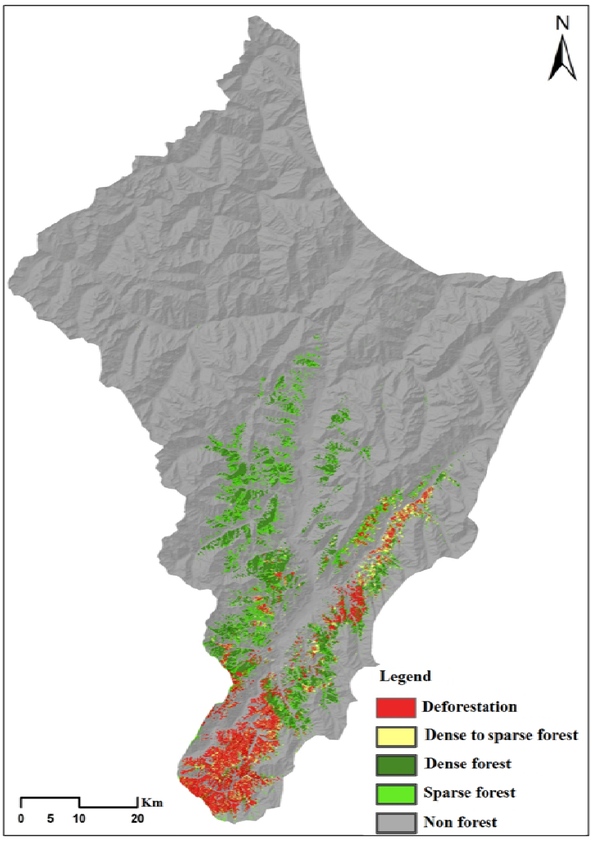

Figure 8 Simulated forest landscape for the year 2030, and change from 2009.

with tropical and boreal regions (Yemshanov and Perera 2002; Cowling et al. 2004). This study is the first one to describe future forest projections in the dry temperate areas of the western Himalayas.

The assessment of forest cover change over two decades revealed ongoing severe deforestation in the Chitral area, with a marked increase in the deforestation rate in 2000–2009, which is particularly alarming. Even taking the 2.5% annual population growth rate into account, the increase in forest loss in the second period suggests that current forest cuttings are beyond local use requirements, and there may be an element of illegal commercial exploitation. The study also showed that there is only a very small area of forest regeneration or restoration.

Analysis of 11 spatially explicit drivers of deforestation using a cellular automaton model revealed a high correlation between neighbourhood deforestation and accessibility (elevation, slope), population density, distance to settlements, and distance to administrative boundary. Forest losses were also related to the two dynamic variables of distance to previous deforestation and distance to previous degradation. In contrast to the global situation, expansion of agriculture did not contribute to the ongoing deforestation in Chitral.

The model achieved an acceptable spatial agreement of 74% with a window size of 11*11 pixels. Timber market dynamics could not be included as a driver due to lack of appropriate data, but might further improve the future model results. A future simulated landscape predicted a further loss of 23% of the existing forest in Chitral tehsil by 2030 if deforestation continues at the present rate. Arandu Union Council, with 2212 households, will be left with only 2070 ha of forest. Due to limited income resources and high poverty, a large part of Chitral's population is dependent on non-timber forest products for their livelihoods, thus continuing deforestation will further worsen their livelihood conditions. Improved conservation efforts to curb deforestation in Chitral are essential, for example by diversifying livelihood options, providing alternative sources of energy, and improving management practices in the area. Our results, with quantitative assessment at union council level, can help in improving management plans for the conservation of these crucial resources.

Acknowledgement

This study is a part of the Himalayan Climate Change Adaptation Programme (HICAP), which is funded by the Ministry of Foreign Affairs, Norway and Swedish International Development Agency (Sida).

The primary datasets were produced under the SERVIR Himalaya Programme supported by the United States Agency for International Development (USAID) and National Aeronautics and Space Administration (NASA).

The boundaries, names, and designations used on the maps do not imply the expression of any opinion whatsoever on the part of ICIMOD concerning the legal status of any country, territory, city or area or of its authorities, or concerning the delimitation of its frontiers or boundaries. The views expressed are those of the authors and do not necessarily reflect those of ICIMOD or the organizations mentioned in the acknowledgements.

References

Adams JB, Sabol DE, Kapos V, et al. (1995) Classification of multispectral images based on fractions of endmembers: Application to land-cover change in the Brazilian Amazon. Remote Sensing of Environment 52(2): 137-154. DOI: 10.1016/0034-4257(94)00098-8

Agarwal C, Green GM, Grove JM, et al. (2002) A review and assessment of land use change models. Dynamics of Space, Time, and Human Choice. CIPEC Collaborative Report Series No.1

Agterberg FP, Bonham-Carter GF (1990) Deriving weights of evidence from geoscience contour maps for the prediction of discrete events. Paper presented at the 22nd APCOM Symposium, Berlin, Germany 2: 381-395.

Ali J, Benjaminsen TA, Hammad AA, et al. (2005) The road to deforestation: An assessment of forest loss and its causes in Basho Valley, Northern Pakistan. Global Environmental Change 15(4): 370-380. DOI: 10.1016/j.gloenvcha.2005.06.004

Almeida CMD, Monteiro AMV, Câmara G, et al. (2005) GIS and remote sensing as tools for the simulation of urban landuse change. International Journal of Remote Sensing 26(4): 759-774.

Beg AR, Bakhsh I (1974) Vegetation of scree slopes in Chitral Gol. The Pakistan Journal of Forestry 24(2): 393-402. DOI: 0.1080/01431160512331316865

Benedethi ACP (2010) Dynamic modeling to simulate changes in forest cover of the Sierras Southeast and Southern Campaign of the Rio Grande South. Tese (Doutorado em Engenharia Florestal) – Universidade Federal de Santa Maria, Santa Maria. pp 166-178.

Bonham-Carter GF (1994) Geographic information systems for geoscientists: modelling with GIS (Vol. 13). Elsevier, Netherlands. pp 33-47

Bürgi M, Hersperger AM, Schneeberger N (2004) Driving forces of landscape change—current and new directions. Landscape ecology 19(8): 857-868. DOI: 10.1007/s10980-004-0245-8

Champion HG, Seth SK, Khattak GM (1966) Forest Types of Pakistan. The Pakistan Forest Institute, Peshawar, Pakistan.

Chadha SK (1988) Himalayas, Ecology and Environment, Mittal Publication, New Dehli, India.

Chavez PS (1996) Image-based atmospheric corrections-revisited and improved. Photogrammetric Engineering and Remote Sensing 62(9): 1025-1035.

Chomitz KM, Thomas TS (2003) Determinants of land use in Amazonia: a fine-scale spatial analysis. American Journal of Agricultural Economics 85(4): 1016-1028. DOI:10.1111/1467-8276.00504.

Cowling SA, Betts RA, Cox PM, et al. (2004) Contrasting simulated past and future responses of the Amazonian forest to atmospheric change. Philosophical Transactions of the Royal Society of London. Series B: Biological Sciences 359(1443): 539-547. DOI: 10.1098/rstb.2003.1427.

FAO (2010) Food and Agriculture Organization. Global forest resources assessment. Rome, Italy. pp: 225. Available online: http://www.fao.org/docrep/013/i1757e/i1757e.pdf. (Accessed on 31 July 2014)

Farfán M, Mas JF, Osorio L (2012) Interpolating socioeconomic data for the analysis of deforestation: a comparison of methods. Journal of Geographic Information System 4: 358-365. DOI: 10.4236/jgis.2012.44041

Fearnside PM, Leal N, Fernandes FM (1993) Rainforest burning and the global carbon budget: Biomass, combustion efficiency, and charcoal formation in the Brazilian Amazon. Journal of Geophysical Research: Atmospheres 98(D9): 16733-16743. DOI: 10.1029/93JD01140.

Ferrari R (2008) Dynamics of Land Use and Cover Modeling the Quarta Colônia Dissertação (Mestrado em Geomática) – Universidade Federal de Santa Maria, Santa Maria, Brazil. p 130.

Gautam AP, Shivakoti GP, Webb EL (2004) Forest cove change, physiography, local economy, and institutions in a mountain watershed in Nepal. Environmental Management 33: 48-61.

Geist HJ, Lambin EF (2001) What drives tropical deforestation? LUCC Report Series No. 4, CIACO, Louvain-la-Neuve, Belgium. p 116. Available online: http://www.pik-potsdam.de/~luedeke/lucc4.pdf. (Accessed on 31 July 2014).

Geist HJ, Lambin EF (2002) Proximate causes and underlying driving forces of tropical deforestation: Tropical forests are disappearing as the result of many pressures, both local and regional, acting in various combinations in different geographical locations. BioScience 52(2): 143-150. DOI: 10.1641/0006-3568(2002)052

Geri F, Amici V, Rocchini D (2011) Spatially-based accuracy assessment of forestation prediction in a complex Mediterranean landscape. Applied Geography 31(3): 881-890. DOI: 10.1016/j.apgeog.2011.01.019

Gong P, Pu R, Biging GS, et al. (2003) Estimation of forest leaf area index using vegetation indices derived from Hyperion hyperspectral data. IEEE Transactions on Geoscience and Remote Sensing 41(6): 1355-1362. DOI: 10.1109/TGRS.2003.812910.

Goodacre AK, Bonham-Carter GF, Agterberg FP et al. (1993) A statistical analysis of the spatial association of seismicity with drainage patterns and magnetic anomalies in western Quebec. Tectonophysics 217(3): 285-305. DOI: 10.1016/0040-1951(93)90011-8.

GoP (2004) National Forest and Rangeland Resource Assessment, Government of Pakistan, Pakistan Forest Institute, Peshawar, Pakistan. pp 56-70

GoP (2010) Annual Agriculture Census Report 2010. Government of Pakistan, Lahore, Pakistan. pp 258. Available online:http://www.pbs.gov.pk/content/agricultural-statistics-pakistan-2010-11. (Accessed on 31 July 2014)

GoP (2002) Government of Pakistan, Pakistan Water Sector Strategy, Ministry of Water and Power. Office of the Chief Engineering Advisor 1, October 2002. p 210. Available online: http://waterinfo.net.pk/?q=wss. (Accessed on 31 July 2014)

GoP (1992) Government of Pakistan, Forestry Sector Master Plan. National Perspective Ried, Collins and Associates, Canada and Silviconsult Ltd. Sweden. Ministry of Food and Agriculture, Islamabad, Pakistan, pp 95.

Henders S, Ostwald M (2012) Forest carbon leakage quantification methods and their suitability for assessing leakage in REDD. Forests 3(1): 33-58. DOI: 10.3390/f3010033

Hosonuma N, Herold M, De Sy V, et al. (2012) An assessment of deforestation and forest degradation drivers in developing countries. Environmental Research Letters 7(4): 7-9. DOI: 10.1088/1748-9326/7/4/044009

Joshi PK, Gairoal S (2004) Land cover dynamics in Garhwal Himalayas—a case study of Balkhila sub- watershed. Journal of the Indian Society of Remote Sensing 32(2): 199-208. DOI: 10.1007/BF03030876.

Joshi PK, Singh S, Agarwal S, et al. (2001) Forest cover assessment in western Himalayas, Himachal Pradesh using IRS 1 C/1 D WiFS data. Current Science 80(8): 941-947. DOI: 10.1007/BF03030776

Kamusoko C, Oono K, Nakazawa A, et al. (2011) Spatial simulation modelling of future forest cover change scenarios in Luangprabang province, Lao PDR. Forests 2(3): 707-729. DOI: 10.3390/f2030707

Kardoulas NG, Bird AC, Lawan AI (1996) Geometric correction of SPOT and Landsat imagery: a comparison of map-and GPS-derived control points. Photogrammetric Engineering and Remote Sensing 62(10): 1173-1177. DOI: 10.1080/01431160701592452

Kennedy RE (2009) Remote sensing change detection tools for natural resource managers: Understanding concepts and tradeoffs in the design of landscape monitoring projects. Remote Sensing of Environment 113(7): 1382-1396. DOI: 10.1016/j.rse.2008.07.018

Keuchel J, Naumann S, Heiler M, et al. (2003) Automatic land cover analysis for Tenerife by supervised classification using remotely sensed data. Remote Sensing of Environment 86(4): 530-541. DOI: 10.1016/S0034-4257(03)00130-5

Khan AA (1975) Report on the wildlife of Chitral. NWFP Forest Department, Peshawar, Pakistan.

Khan AM (1994) Culture and natural resources of Kalash valley Bomburet. M.Sc, University of Peshawar, Pakistan.

Sheikh MI, Khan M (1983) Forestry and range management in Chitral District. Pakistan Journal of Forestry 33(3): 105-110

Knudsen A, Madsen ST (1999) Deforestation and Entrepreneurship in the North-West Frontier Province, Pakistan. State, Society and the Environment in South Asia, Curzon, London. pp 200-235.

Kutrib M, Vollmar R, Worsch TH (1997) Introduction to the special issue on cellular automata. Parallel Computing 3(11): 44-66. DOI: 10.1016/S0167-8191(97)00079-3

Lodhi MA, Echavarria FR, Keithley C (1998) Using remote sensing data to monitor land cover changes near Afghan refugee camps in northern Pakistan. Geocarto International 13(1): 33-39. DOI: 10.1080/10106049809354626

Maeda EE, Almeida CM, Carvalho Ximenes A, et al. (2011) Dynamic modeling of forest conversion: Simulation of past and future scenarios of rural activities expansion in the fringes of the Xingu National Park, Brazilian Amazon.

International Journal of Applied Earth Observation and Geoinformation 13(3): 435-446. DOI: 10.1016/j.jag.2010.09.008

Nüsser M (2000) Change and persistence: Contemporary landscape transformation in the nanga parbat region, northern Pakistan. Mountain Research and Development 20: 348-355. DOI: 10.1659/0276-4741(2000)020[0348:CAPCLT]2.0.CO;2

Pandit MK, Sodhi NS, Koh LP et al. (2007) Unreported yet massive deforestation driving loss of endemic biodiversity in Indian Himalaya. Biodiversity and Conservation 16(1): 153-163. DOI: 10.1007/s10531-006-9038-5

Pontius RG (2002) Statistical methods to partition effects of quantity and location during comparison of categorical maps at multiple resolutions. Photogrammetric Engineering and Remote Sensing 68(10): 1041-1050.

Qamer FM, Abbas S, Saleem R, et al. (2012) Forest cover change assessment in conflict-affected areas of northwest pakistan: The case of swat and shangla districts. Journal of Mountain Science 9: 297-306. DOI: 10.1007/s11629-009-2319-1

Qasim M, Hubacek K, Termansen M, et al. (2011) Spatial and temporal dynamics of land use pattern in district swat, Hindu Kush Himalayan region of Pakistan. Applied Geography 31: 820-828. DOI: 10.1016/j.apgeog.2010.08.008

Rademaekers K, Eichler L, Berg J, et al. (2010) Study on the evolution of some deforestation drivers and their potential impacts on the costs of an avoiding deforestation scheme; ECORYS and IIASA: Rotterdam, Netherlands.

Rogan JFJ, Roberts DA (2002) A comparison of methods for monitoring multitemporal vegetation change using thematic mapper imagery. Remote Sensing of Environment 80: 143-156. DOI: 10.1016/S0034-4257(01)00296-6

Rozenstein O, Karnieli A (2011) Comparison of methods for land-use classification incorporating remote sensing and GIS inputs. Applied Geography 31:533-544.DOI: 10.1016/j.apgeog.2010.11.006

Schickhoff U (1995) Himalayan forest-cover changes in historical perspective: A case study in the Kaghan valley, Northern Pakistan. Mountain Research and Development 3-18. DOI: 10.2307/3673697

Soares-Filho BS, Coutinho CG, Lopes PC (2013) Dinamica—a stochastic cellular automata model designed to simulate the landscape dynamics in an amazonian colonization frontier. Ecological modelling 154: 217-235. DOI: 10.1016/S0304-3800(02)00059-5

Soares-Filho BS, Nepstad DC, Curran LM, et al. (2006) Modelling conservation in the amazon basin. Nature 440: 520-523. DOI: 10.1038/nature04389

Shroder JF (1998) Slope failure and denudation in the western Himalaya. Geomorphology 26(1): 81-105. DOI: 10.1016/S0169-555X(98)00052-X

Swaminathan MS (1988) The promise of agroforestry for ecological and nutrition security. The potential of agroforestry. World Agroforestry Center, Nairobi, Kenya.

Tejwani K (1990) Bio-Physical and socio-economic causes of land degradation and strategy to foster watershed rehabilitation in the Himalayas. in Sah N, Bhatt S, and Pande R (eds.). Himalaya: Environment, Resources and Development, pp. 378-85. Shree Almora Book Depot, Almora, India.

Tekle K (2000) Land-cover changes between 1958 and 1986 in Kalu district, Southern Wello, Ethiopia. Mountain Research and Development 20: 42-51. DOI: 10.1659/0276-4741(2000)020[0042:LCCBAI]2.0.CO;2

Tole L (1998) Sources of deforestation in tropical developing countries. Environmental Management 22: 19-33. DOI: 10.1016/j.worlddev.2005.09.005

Verburg PH, De Koning GHJ, Kok K, et al. (1999) A spatial explicit allocation procedure for modelling the pattern of land use change based upon actual land use. Ecological Modelling 116: 45-61. DOI: 10.1016/S0304-3800(98)00156-2

Walker RT (1987) Land use transition and deforestation in developing countries. Geographical Analysis 19: 18-30. DOI: 10.1111/j.1538-4632.1987.tb00111.x

Wolfram S (1983) Cellular automata. Los Alamos Science 9: 2–27. Available online: http://www.stephenwolfram.com/publications/cellular-automata-complexity/pdfs/cellular-automata.pdf (Accessed on 31 July 2014).

Yemshanov D, Perera AH (2002) A spatially explicit stochastic model to simulate boreal forest cover transitions: general structure and properties. Ecological Modelling 150: 189-209. DOI: 10.1016/S0304-3800(01)00480-X